Stochastic Algorithms for Controller Optimization of Grid Tied Hybrid AC/DC Microgrid with Multiple Renewable Sources

Pramod Bhat NEMPU, Jayalakshmi Narayana SABHAHIT
Electrical and Electronics Engg., Manipal Institute of Technology, Manipal
Manipal Academy of Higher Education, Manipal, India – 576104
jayalakshmi.ns@manipal.edu

***Abstract*—The hybrid AC/DC microgrid (MG) configuration is efficient as it reduces the need for multiple power conversions and hence losses. Therefore, this paper focuses on the study of grid assisted hybrid AC/DC MG comprising of solar PV and fuel cell (FC) systems on DC subgrid with supercapacitor (SC) as the short term storage device and wind energy conversion system (WECS) on the AC subgrid. A comprehensive study of the operation of MG is performed under varying system conditions in MATLAB/Simulink software. The real and reactive power (PQ) control scheme is used to regulate the DC bus voltage and power flow between the subgrids. Genetic algorithm (GA), artificial bee colony (ABC) optimization, particle swarm optimization (PSO) and the PSO with new update mechanism (PSOd) are used to compute the optimum gain values of proportional-integral (PI) controller in the PQ control scheme. The SC bank effectively reduces the power stress on the subgrids of the proposed hybrid MG system during intermittent conditions of load and generation. In addition, a comparative study of the heuristic optimization techniques is presented in detail. The ABC algorithm is found to arrive at the best results in determining the optimal gains of PI controller.**

***Index Terms*—fuel cells, heuristic algorithms, microgrid, renewable energy sources, supercapacitors.**

I. Introduction

A MG is the combination of renewable sources, consumers and energy storage devices that operate with or without the assistance of electric utility. Generally, voltage source converters (VSC) are employed for facilitating the exchange of power with the grid. MGs can operate in three distinct configurations. AC MGs have been explored broadly due to the fact that interfacing them with the utility is simpler. Conversely, most renewable sources produce DC power and modern loads work on DC thus DC MGs are advantageous. A useful and multifaceted architecture is called hybrid AC/DC MG which includes the benefits of DC and AC systems [1-3].

Several works of literature have discussed different control techniques for grid independent operation of hybrid MGs. In [4], a normalization based control technique for the interlinking converter (ILC) is discussed. The current reference required for active power exchange is computed by taking the difference between normalized values of frequency and DC bus voltage. The same control scheme is modified, experimentally analyzed and presented in [5, 6]. The normalization based control scheme is enhanced in [7]. An improved droop control technique with two stages is proposed in [8]. Different droop control schemes for hybrid MGs are reviewed in [9]. A PI controller based novel perturb and observe (PI-PO) control algorithm for maximum power point tracking (MPPT) in a PV, WECS and FC based stand-alone hybrid AC/DC MG is proposed in [10] and is proved to be effective as compared to traditional PO MPPT.

A solid oxide fuel cell assisted WECS is analyzed in grid-connected mode with SCs in DC coupled MG structure in [11]. A study on control schemes for power regulation of hybrid MGs with the energy storage device is presented for isolated and grid integrated operating modes in [12] and experimental validation is made using pulsed loads. A grid assisted hybrid AC/DC MG with PV, battery and FC on DC side, WECS, microturbine and diesel engine on AC side is studied in [13] and D-FACTS is used for enhancing the system performance. PSO optimized PID controllers are used in D-FACTS.

In [14], a fuzzy logic controller (FLC) based dynamic voltage restorer (DVR) is discussed and real coded GA is used for FLC to mitigate voltage sags/swells in a distribution system. PSO was introduced for the first time in [15]. A PV, FC and battery hybrid system with FLC is studied in [16] and different optimization techniques like imperialist competitive algorithm (ICA), PSO, cuckoo search algorithm, ant colony optimization (ACO) and quantum behaved PSO (QPSO) are compared and ICA and QPSO are found to outperform other techniques. An application of PSO as S-function in the FLC of grid tied PV inverter's control scheme is proposed in [17]. In [18], various nature-inspired population based algorithms are used to determine optimal controller gains in a PID controller of robot arm control mechanism. PSO gave better results as compared to differential evolution (DE), GA, bat and hybrid bat algorithms (BA and HBA) and cuckoo search (CS) algorithm. In [19], the controller of a robot is optimized using different modifications of DE. A PV and FC based AC coupled MG is analyzed in both grid dependent and grid independent modes using PQ controller and droop controller respectively. ABC is used to obtain optimal controller gain values in the PQ controller and its effectiveness are evaluated as compared to manual tuning technique [20]. A DC coupled grid connected PV, WECS and FC based MG is discussed in [21] and PSO is used to tune the controller of inverter both offline and online considering error and integral time absolute error as performance indices and the results are compared. An improved PSO is proposed with a new update rule by

Digital Object Identifier 10.4316/AECE.2019.02007

eliminating the velocity update rule in [22]. This is compared with several other variants of PSO, firefly algorithm (FA), CS algorithm and glowworm swarm optimization (GSO) algorithm and PSOd is found to be better in many cases. The mathematical modelling of the ILC with PQ control scheme is described in [23, 24]. The application of FLC in inverter control scheme for grid independent operation of PV-FC hybrid system is discussed in [25].

From the literature review, it is found that PV, WECS and FC based hybrid systems have not been analyzed in hybrid AC/DC coupled structure with SC bank. The appropriateness of PSOd algorithm in controller gain optimization is not yet explored in the literature. There is no comparative study in the literature on few optimization techniques like ABC, GA and PSO as applied to controller optimization; however, they are individually used in different articles for controller tuning. The performance of PSOd has not been evaluated in comparison with effective optimization methods like GA and ABC. The research contributions of this article are as follows.

- In depth study of PV-WECS-FC based hybrid AC/DC MG with grid support under dynamically varying conditions of power generation and load demand.
- Verification of the importance of SC bank in the proposed hybrid AC/DC MG system.
- The comparative study of stochastic optimization techniques in optimizing the controller gains.

In this article, section 2 provides the details of the MG system and the control schemes of FC stack and SC bank. In section 3, the control scheme of ILC is described and in section 4, different optimization techniques used in the work are briefly explained. The results of simulation are analyzed in section 5 and the inferences are given in section 6.

II. Hybrid AC/DC MG

The schematic illustration of the hybrid MG considered for the study with control schemes of FC stack and SC bank is in Fig. 1. This section gives brief description of the configuration of MG and the control schemes of FC stack and SC bank.

A. *Configuration of hybrid AC/DC MG*

In this system, a PV array of capacity 21.7 kW is taken as the main source in DC subgrid and PMSG based WECS of capacity 40 kW is the power source for AC subgrid. The FC stack is the auxiliary source for DC subgird. The SC bank of capacity 4F and 400 V helps in compensating for the power variation produced by intermittency occurring on both the subgrids. A dynamic model of PV array is realized [26]. The model of FC is realized as described in [27]. The PV system comprises of incremental conductance (IC) MPPT algorithm realized using boost converter [26] for extracting the power conforming to the maximum power point. The WECS has a diode bridge rectifier for converting AC output of PMSG to DC power and a boost converter for extracting maximum power using perturb and observe (P&O) algorithm [28]. Then the boost converter's output is inverted and fed to the AC bus through a filter. The inverter of WECS is controlled by PQ controller similar to that of ILC as it is connected to grid coupled AC bus [20]. The AC bus is tied to 100 MVA, 3.3 kV, and 50 Hz utility grid through a transformer. Both the subgrids are coupled by a bidirectional ILC which is controlled by PQ control scheme.

B. *Control schemes of FC system and SC bank*

The FC system has a current controlled boost converter which decides the power production from FC as per the load requirements on the DC subgrid when the DC load current (I_L) exceeds the current output of the PV array (I_{PV}). The difference between DC load current and the current output of PV system acts as the reference current to the controller. The output current of FC system (I_{FC}) is taken as feedback and a PI regulator decides the duty ratio of the boost converter. When the output of PV system exceeds the demand, surplus in generation is sent to the grid via the ILC. The SC system has a bidirectional DC/DC converter with a voltage-current (V-I) control scheme [26] consisting of two control loops. The outer loop takes the voltage of DC subgrid (V_{dc}) as the feedback and compares it with the reference voltage of 800 V and the FLC computes the current reference of SC bank. (I_{SC}). The inner loop takes I_{SC} as feedback and computes duty ratio via a PI regulator. This helps in managing sudden variations on both the subgrids.

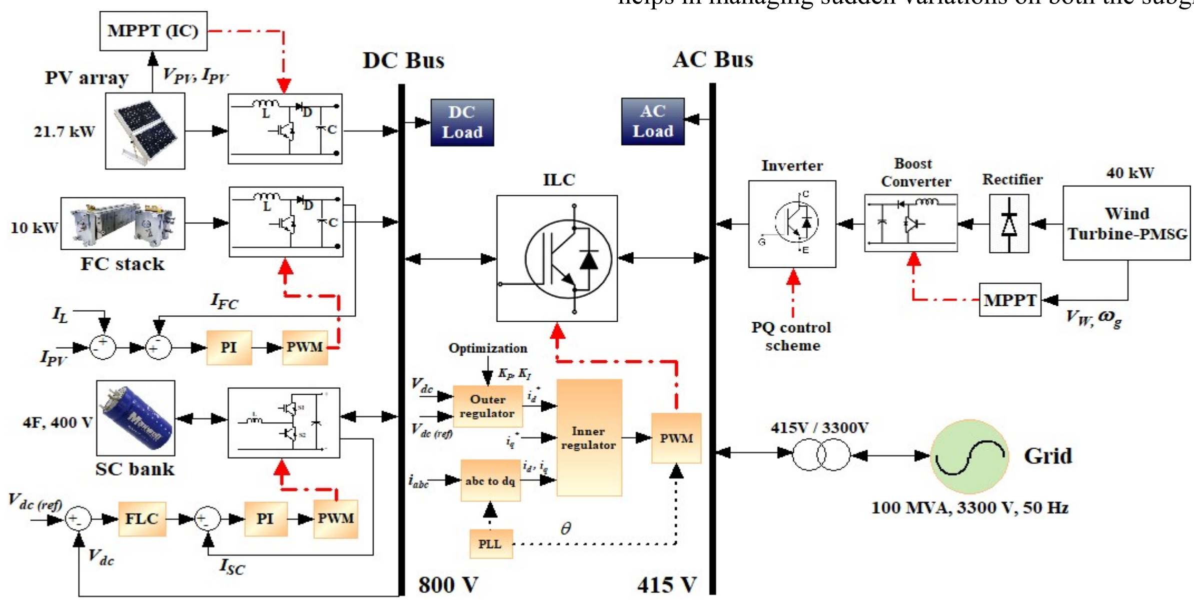

Figure 1. Block diagram of hybrid AC/DC MG

III. Control Strategy of ILC

The ILC is coupled to the AC bus via a LCL filter. PQ controller is responsible for maintaining the constant voltage at DC bus and facilitating appropriate power flow between the subgrids. The control technique is depicted in Fig. 2. The three phase instantaneous power is given by equation (1).

$$P(t) = v_a i_a + v_b i_b + v_c i_c \tag{1}$$

Real power (P) and reactive power (Q) are given by equations (2) and (3) respectively [28].

$$P = \frac{3}{2}\left(v_d i_d + v_q i_q\right) \tag{2}$$

$$Q = \frac{3}{2}(v_q i_d - v_d i_q) \tag{3}$$

If the reference frame and grid voltage are synchronized, then P and Q are given by equations (4) and (5).

$$P = 1.5(v_d i_d) \tag{4}$$

$$Q = 1.5(v_d i_q) \tag{5}$$

The exchange of P and Q among the subgrids is managed by adjusting the direct (d) and quadrature (q) axis currents i_d and i_q respectively. This control system has an outer loop that maintains the voltage at DC subgrid and an inner loop that controls d and q axis currents [11, 28]. The $i_{q\ (ref)}$ is set to zero maintaining unity power factor (UPF).

The phase locked loop (PLL) computes the phase angle of grid voltage to synchronize ILC with grid. If R and L are the total filter resistance and inductance respectively and ω is the angular frequency, the relationship representing the voltage balance across the filter in terms of d and q axis voltages v_d and v_q can be expressed as in (6).

$$\begin{bmatrix} v_d^1 \\ v_q^1 \end{bmatrix} = R\begin{bmatrix} i_d \\ i_q \end{bmatrix} + L\frac{d}{dt}\begin{bmatrix} i_d \\ i_q \end{bmatrix} + L\begin{bmatrix} 0 & -\omega \\ \omega & 0 \end{bmatrix}\begin{bmatrix} i_d \\ i_q \end{bmatrix} + \begin{bmatrix} v_d \\ v_q \end{bmatrix} \tag{6}$$

The open loop transfer functions of the outer and inner loop of the PQ controller ignoring disturbance are given by equations (7) and (8) respectively [23, 24].

$$G_{V(OL)} = \left(K_p + \frac{K_i}{s}\right)\left(\frac{1}{T_{eq}s+1}\right)\left(\frac{3}{2}\frac{v_d}{v_{dc}}\right)\left(\frac{1}{Cs}\right) \tag{7}$$

$$G_{C(OL)} = \left(K_p + \frac{K_i}{s}\right)\left(\frac{1}{T_a s+1}\right)\left(\frac{1}{R}\right)\left(\frac{1}{\tau s+1}\right) \tag{8}$$

Where T_a and T_{eq} are the functions of switching frequency of the ILC and τ is the time constant defined as the ratio of filter inductance to its resistance as expressed by equations (9), (10) and (11).

$$T_a = \frac{1}{2f_{sw}} \tag{9}$$

$$T_{eq} = 2T_a \tag{10}$$

$$\tau = \frac{L}{R} \tag{11}$$

Where K_p and K_i are proportional and integral gains respectively. f_{sw} is the switching frequency, C is the capacitance of DC link. The ratio of v_d and V_{dc} is usually unity. [24]. The PI controllers employed in this control scheme are tuned initially by trial and error (manual tuning) method. In Table I, the values of different parameters of the transfer function of PQ control scheme are provided.

Table I. Different Parameters of Transfer Function

Parameters	Values
R	0.04 Ω
L	2.4 mH
C	5 mF
f_{sw}	10 kHz

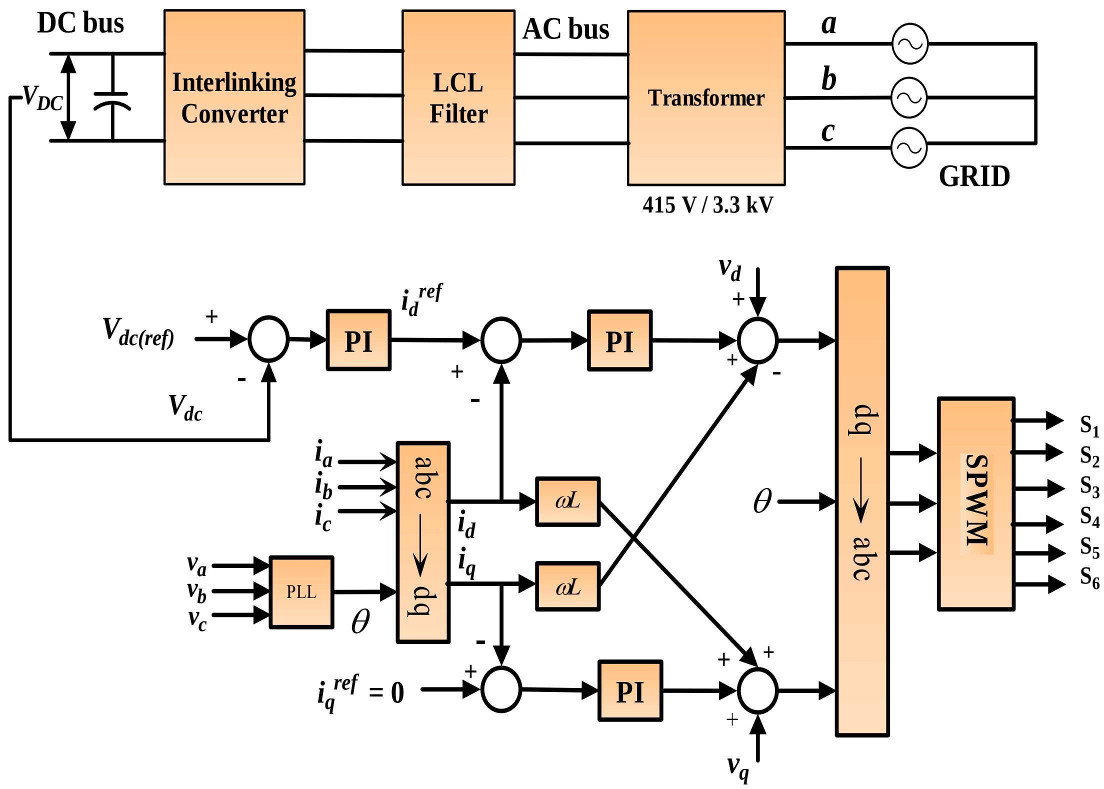

Figure 2. PQ control scheme of ILC

IV. Tuning of PI Controller Using Optimization Techniques

The outer loop of PQ controller is optimized offline to minimize the cost function by different stochastic optimization techniques considering integral time absolute error (*ITAE*) as the performance criterion or the cost function as represented in Fig. 3. Inner loop has varying reference and the outer loop has fixed voltage reference and hence the outer loop controller is optimized for the convenience of analysis. *ITAE* is expressed as in (12).

$$ITAE = \int_0^T t.\left|e(t)\right|.dt \tag{12}$$

The error (e) is computed based on the step response of the system. *ITAE* can also be expressed as in equation (13).

$$ITAE = \sum_0^T t.\left|e\right|.\Delta t \tag{13}$$

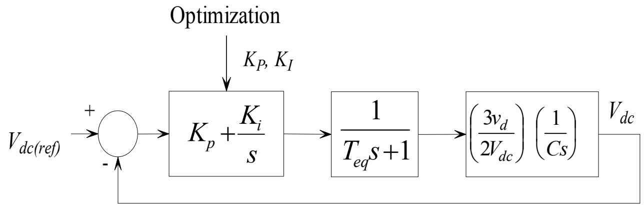

Figure 3. PQ controller loop representing optimization

A. Genetic algorithm

GA is a heuristic optimization algorithm based on genetics and natural selection [29]. It uses random search for solving optimization problems [14, 18]. GA uses a search space with a collection of randomly generated solutions called population. Individual solutions are called chromosomes. Thus a chromosome comprises of genes (variables). A fitness value is given for every solution signifying its goodness. The individual with the optimal fitness is taken. The GA aims to produce better solutions by combining parent solutions. This is called crossover. To ensure that the best solution is not missed, genes are altered to create new solutions. This is called mutation. Consequently, good solutions are made to reproduce, so that offspring receives features from good parent solution. The flow chart of GA is shown in Fig. 4.

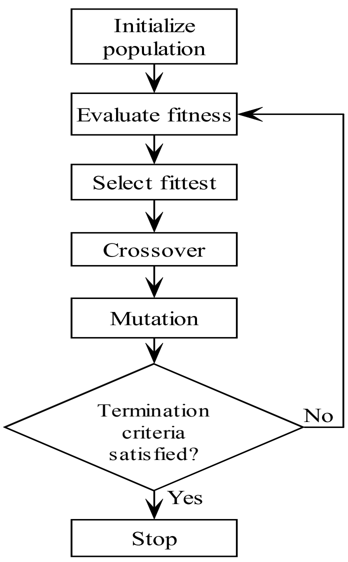

Figure 4. Flowchart of GA

B. Particle swarm optimization

The PSO simulates the behaviour of bird groups. It is population based and its population involves particles each representative of the solution [15]. The PSO algorithm discovers a new solution based on the movement of particles in the search space in the path of the present best solution [21, 22]. The flowchart of the PSO is given in Fig. 5.

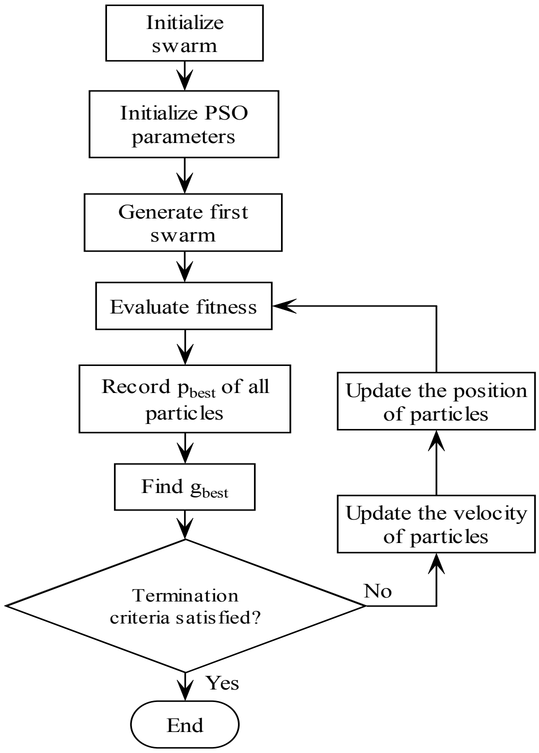

Figure 5. Flowchart of PSO algorithm

If X is the particle, V is the velocity, L and U are the lower and upper boundaries of the particles, r is the random number, N is the number of particles and D is the dimension of the search space, then initial position and velocity are expressed as in equations (14) and (15) respectively [22].

$$X_{i,j}(0) = L_j + r_i^j (U_j - L_j), i = 1,2...N \; and \; j = 1,2...D \tag{14}$$

$$V_{i,j}(0) = \{L_j + r_i^j (U_j - L_j) - X_{i,j}(0)\}/2 \tag{15}$$

The population has a personal best for each particle (P_{best_i}) and a global best (g_{best}). The initial value of personal best is expressed as in (16).

$$P_{best_i}(0) = X_i(0) \tag{16}$$

The best solution in the initialized phase is given by (17)

$$g_{best} = arg\ min\ (\ f(\ p_{best_i}\ )) \tag{17}$$

The velocity update rule is given by equation (18).

$$\begin{aligned} V_{i,j}(t+1) = wV_{i,j}(t) + r_{i,j}^1 c_1 \left\{p_{besti,j}(t) - X_{i,j}(t)\right\} \\ + r_{i,j}^2 c_2 \left\{g_{best j}(t) - X_{i,j}(t)\right\} \end{aligned} \tag{18}$$

Based on new velocity, new particle position can be computed as per equation (19).

$$X_{i,j}(t+1) = X_{i,j}(t) + V_{i,j}(t+1) \tag{19}$$

Based on the new position, personal best is computed for each particle using equation (20).

$$p_{best_i}(t+1) = \begin{cases} X_i(t+1) \; if \; f\left(X_i(t+1)\right) \; is \; better \; than \; p_{best_i}(t) \\ p_{best_i}(t) \qquad otherwise \end{cases} \tag{20}$$

C. PSO with new update rule

The PSOd algorithm is proposed in [22]. The velocity update rule is eliminated and a new rule based on normal distribution is introduced. The flowchart of PSOd is in Fig. 6.

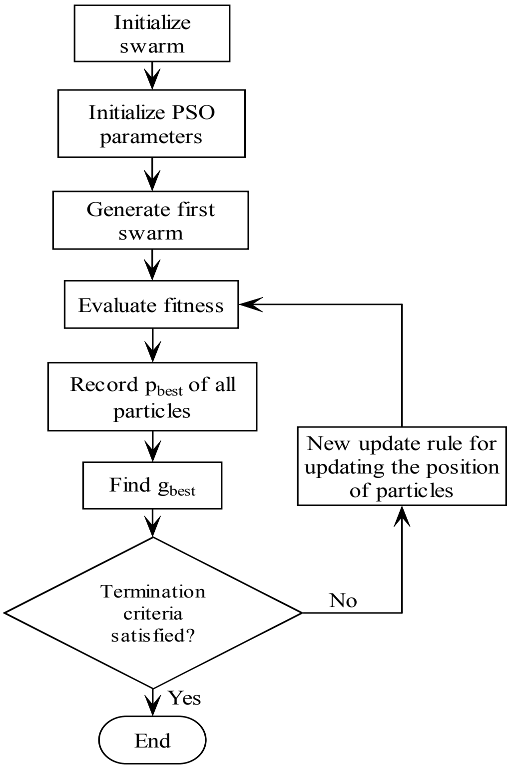

Figure 6. Flowchart of PSOd algorithm

If μ is the mean and σ is the standard deviation, then the new position can be computed using equations (21), (22), (23) and (24).

$$X_{i,j}(t+1)=\mu+\sigma\times z \quad (21)$$

$$\mu=(X_{i,j}(t)+p_{best_{i,j}}(t)+g_{best_j}(t))/3 \quad (22)$$

$$\sigma=\sqrt{\frac{1}{3}\times\{(X_{i,j}(t)-\mu)^2+(p_{best_{i,j}}(t)-\mu)^2+(g_{best_j}(t)-\mu)^2\}} \quad (23)$$

$$z=(-2\ln(m))^{0.5}\times\cos(2\pi n) \quad (24)$$

Where m and n are the uniform random numbers in the range [0, 1].

D. Artificial bee colony optimization

In ABC, so as to discover the global best, artificial bees search in a search space [20, 30]. The three groups of bees are: employed bees (EB), onlookers (OL) and scouts. They search for food sources or solutions. The ABC algorithm is shown in Fig. 7. Initial solution $X_i = \{X_{i,1}, X_{i,2}, \ldots X_{i,D}\}$ is created randomly based on equation (25).

$$X_{i,j}=X_j^{\min}+r(X_j^{\max}-X_j^{\min}) \; i=1,2..SN \; and \; j=1,2..D \quad (25)$$

Where SN represents the EB which is equal to the number of OLs, D represents the number of optimization variables, $X_j^{\min}$ and $X_j^{\max}$ are the limits of j and r is the random number in (0, 1). To search the solutions in solution space, a solution vector $V_{i,j}$ is computed using (26).

$$V_{i,j}=X_{i,j}+\varphi_{i,j}(X_{i,j}-X_{k,j}) \quad (26)$$

Where $\varphi_{i,j}$ is the random number in [-1, +1].

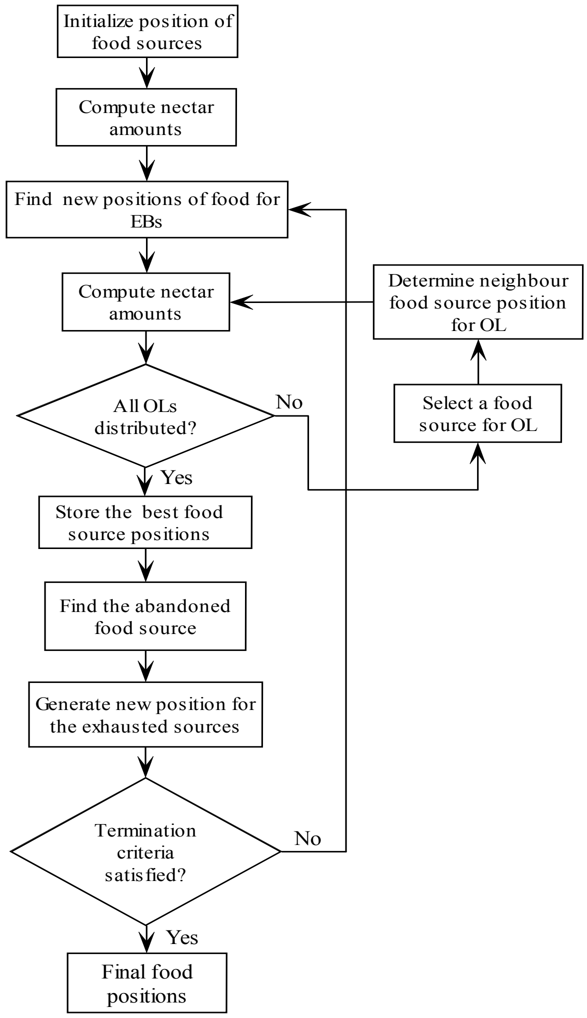

Figure 7. Flowchart of ABC algorithm

V. Results and Discussion

The hybrid AC/DC MG is analyzed for varying load demand on both subgrids with the power output of PV array and WECS varying continuously. PV system produces output in proportion to the irradiance given as input. WECS output is produced in proportion to the cube of wind speed. Fig. 8 shows the demand on DC bus, PV system output, the output of FC system and SC bank. The FC stack supplies power to DC loads when the PV array generates power lesser than the demand. However, FC is not able to produce the power to match the demand immediately with the varying load due to slow dynamics. The SC bank helps in sudden power balance by either absorbing or supplying power during dynamic fluctuations on the subgrids.

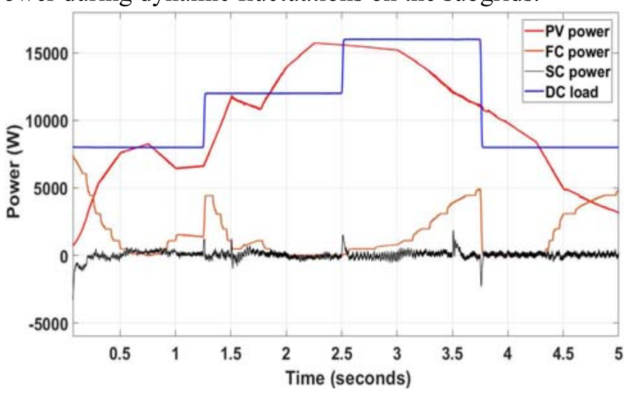

Figure 8. DC load demand, PV power, FC power and power output of SC

The load demand on AC subgrid, power output of WECS and real power exchanged with the utility is shown in Fig. 9. Whenever the WECS output is lesser than the demand, power deficit is drawn from the grid and surplus in the power generated is sent to the grid. The reactive power exchanged with the utility is zero as the reference provided for reactive power exchange is zero which is shown in Fig. 10. The power flow between the subgrids is depicted in Fig. 11. When the output of PV array exceeds the demand, additional power produced in DC subgrid is transferred to the AC subgrid via the ILC.

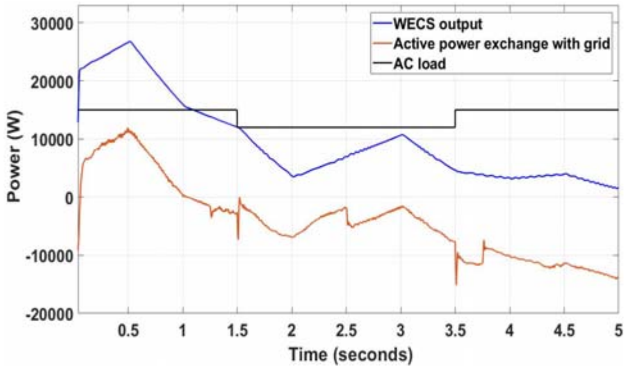

Figure 9. AC load demand, WECS output power and the grid active power

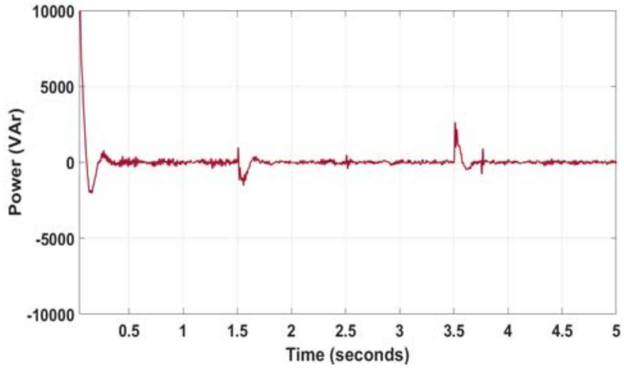

Figure 10. Reactive power

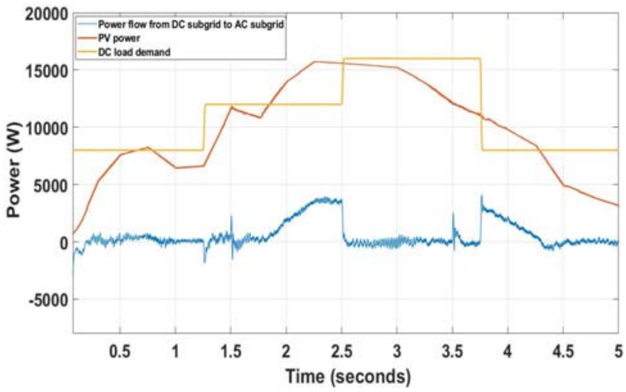

Figure 11. Power flowing between the subgrids

The total power delivered to the DC load with and without the SC bank is shown in Fig. 12. The total power generated in DC subgrid matches with the DC load demand. It can be seen that the transients are managed by SC bank as it is capable of operating fast. Similarly, the plot of real power exchanged with grid is shown in Fig. 13. Sudden power stress on the grid is reduced when SC bank is used in the system. Hence by incorporating the SC bank in the DC subgrid, the slow dynamics of the FC system is compensated and the power fluctuations on both the subgrids of hybrid AC/DC MG are minimized.

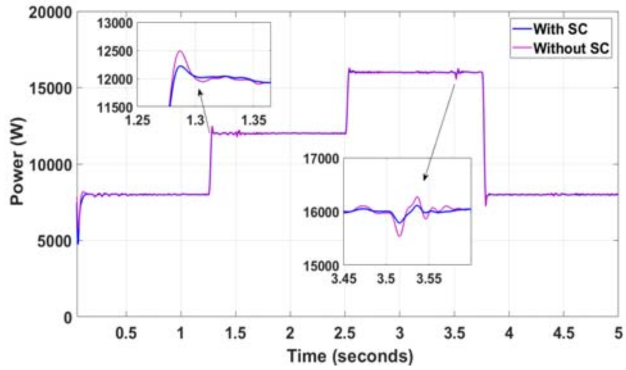

Figure 12. Power supplied to DC load with and without SC

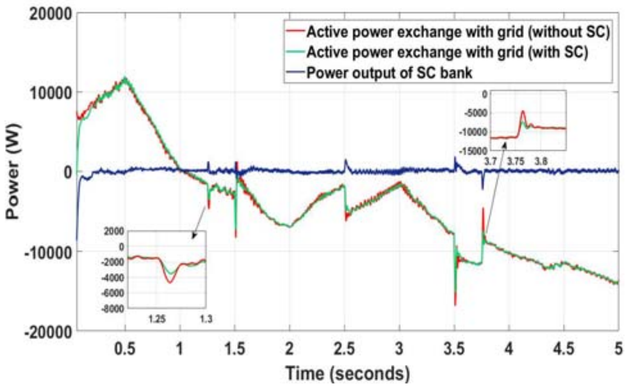

Figure 13. Active power exchanged with the grid with and without SC bank

Initially, the PI regulators in the PQ control scheme are tuned manually. So as to verify the effectiveness of algorithms, the population size of 50 is taken and 50 iterations are considered. The values of controller gains obtained by different stochastic algorithms and corresponding best cost values are given in Table II. ABC has the best cost compared to other techniques and as observable from Table II, the proportional gain has a significant difference when compared with other techniques.

TABLE II. CONTROLLER GAINS AND BEST COST OBTAINED USING DIFFERENT ALGORITHMS

Algorithm	K_P	K_I	Best cost
GA	2.221	835.9	6.26×10^{-8}
PSO	1.997	730.54	4.67×10^{-8}
PSOd	2.122	776.96	2.46×10^{-8}
ABC	8.479	735.8	0.03501×10^{-8}

The plot of best cost vs the number of iterations obtained with different optimization algorithms is shown in Fig. 14. It can be observed that the best cost obtained with ABC is minimum and fast convergence is achieved with PSOd algorithm. Minimal variations are observed in the performance of PSO and PSOd algorithms.

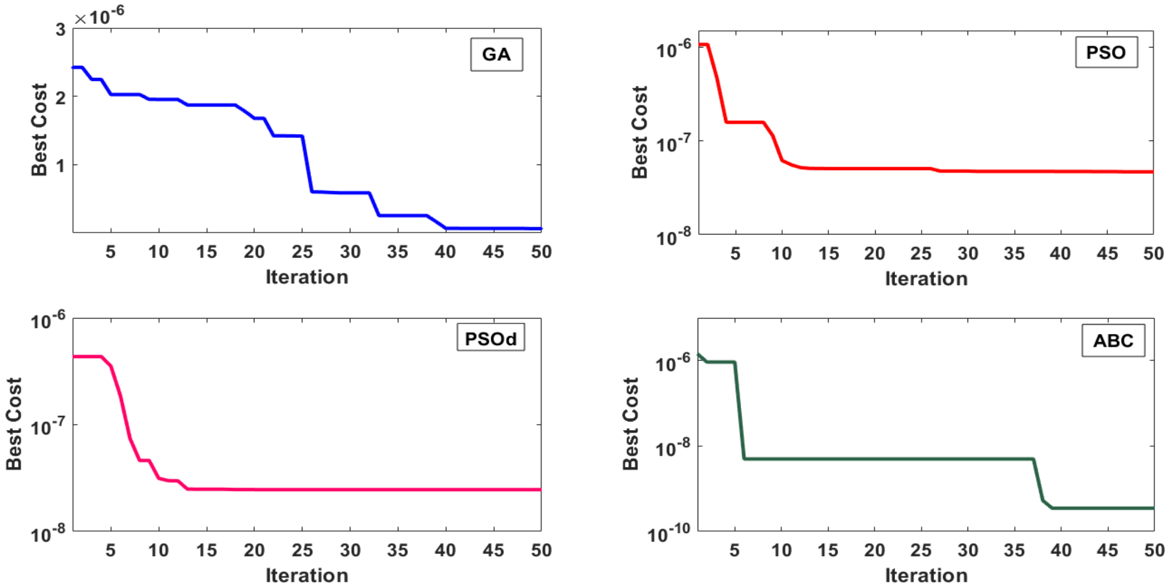

Figure 14. Best cost vs iterations with different algorithms

The voltage at DC bus of the hybrid MG with different algorithms is shown in Fig. 15. It can be seen that the overshoot is high when the GA based PI is used and it is the least when ABC based PI is used. The percentage overshoot values and the settling time are tabulated in Table III. In order to determine the settling time, the time taken by the response to stay and settle within 2 percent error is observed in the DC bus voltage. It can be observed that the overshoot is significantly reduced when the controller gains are optimized by ABC and only small variations are observed in settling time with different optimization techniques. When both settling time and overshoot are evaluated, ABC shows better performance in optimizing the controller parameters.

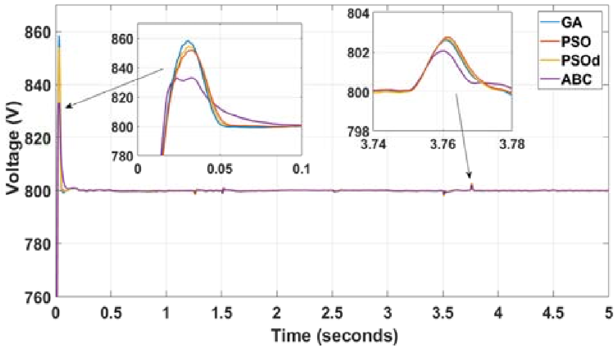

Figure 15. DC bus voltage

TABLE III. COMPARISON OF DIFFERENT ALGORITHMS

Algorithm	Overshoot (%)	Settling time (s)
GA	7.31	0.044
PSO	6.48	0.046
PSOd	6.76	0.045
ABC	4.14	0.045

The waveform of current exchanged between the MG and utility grid is shown in Fig. 16. The LCL filer effectively filters the harmonics generated due to switching. The harmonic spectrum corresponding to the grid current is shown in Fig. 17. It can be observed that the harmonics are within the acceptable limits i.e. less than 5 percent as specified by IEEE standards.

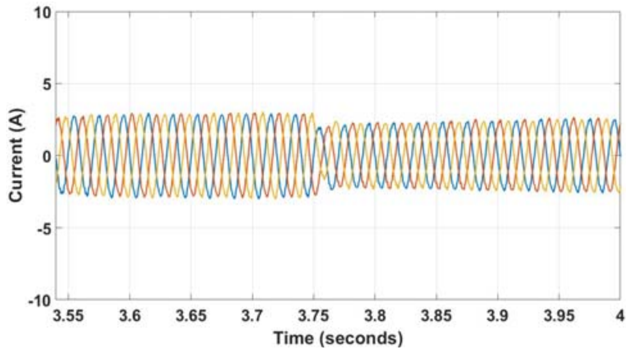

Figure 16. Current exchanged with the utility grid

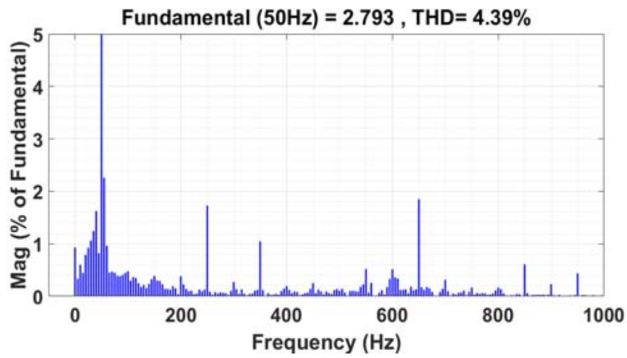

Figure 17. Harmonic spectrum of current exchanged with the utility grid

VI. CONCLUSION

This paper presents the dynamic simulation study of grid tied PV, WECS and FC based hybrid AC/DC MG. The FC system supplies power when the power output of the PV system is lesser than the DC load demand. The SC bank effectively absorbs or provides power when dynamic variations occur in both the subgrids of the proposed MG system. The heuristic optimization techniques such as GA, PSO, PSOd and ABC are used in this work to optimize the PI controller gains in PQ controller. The voltage response with GA has lower settling time, but it has maximum overshoot. The peak overshoot is significantly reduced when the ABC is used for optimization. Overall, ABC is found to have outperformed other algorithms. In the future, this work will be extended by considering the autonomous operation and control of the MG using adaptive controllers.

REFERENCES

[1] X. Liu, P. Wang, P. C. Loh, "A hybrid AC/DC microgrid and its coordination control," IEEE Transactions on Smart Grid, vol. 2, no. 2, pp. 278-286, Jun. 2011. doi:10.1109/TSG.2011.2116162

[2] A. Gupta, S. Doolla, K. Chatterjee, "Hybrid AC–DC microgrid: systematic evaluation of control strategies," IEEE Transactions on Smart Grid, vol. 9, no. 4, pp. 3830-3843, Jul. 2018. doi:10.1109/TSG.2017.2727344

[3] F. Nejabatkhah, Y. W. Li, "Overview of power management strategies of hybrid AC/DC microgrid," IEEE Transactions on Power Electronics, vol. 30, no. 12, pp. 7072-7089, Dec. 2015. doi:10.1109/TPEL.2014.2384999

[4] C. Jin, P. C. Loh, P. Wang, Y. Mi, F. Blaabjerg, "Autonomous operation of hybrid AC-DC microgrids," in IEEE International Conference on Sustainable Energy Technologies (ICSET), Kandy, Sri Lanka, Dec. 2010, pp. 1-7. doi:10.1109/ICSET.2010.5684456

[5] P. C. Loh, D. Li, Y. K. Chai, F. Blaabjerg, "Autonomous control of interlinking converter with energy storage in hybrid AC–DC microgrid," IEEE Transactions on Industry Applications, vol. 49, no. 3, pp. 1374-1382, May. 2013. doi:10.1109/TIA.2013.2252319

[6] P. C. Loh, D. Li, Y. K. Chai, F. Blaabjerg, "Autonomous operation of hybrid microgrid with AC and DC subgrids," IEEE Transactions on Power Electronics, vol. 28, no. 5, pp. 2214-2223, May. 2013. doi:10.1109/TPEL.2012.2214792

[7] M. Baharizadeh, H. R. Karshenas, J. M. Guerrero, "An improved power control strategy for hybrid AC-DC microgrids," International Journal of Electrical Power & Energy Systems, vol. 95, pp. 364-373, Feb. 2018. doi:10.1016/j.ijepes.2017.08.036

[8] N. Eghtedarpour, E. Farjah, "Power control and management in a hybrid AC/DC microgrid," IEEE transactions on smart grid, vol. 5 no. 3, pp. 1494-1505, May 2014. doi:10.1109/TSG.2013.2294275

[9] S. M. Malik, X. Ai, Y. Sun, C. Zhengqi, Z. Shupeng, "Voltage and frequency control strategies of hybrid AC/DC microgrid: a review," IET Generation, Transmission & Distribution, vol. 11, no. 2, pp. 303-313, Jan. 2017. doi:10.1049/iet-gtd.2016.0791

[10] E. Kabalcı, "An islanded hybrid microgrid design with decentralized DC and AC subgrid controllers," Energy, vol. 153, pp.185-199, Jun. 2018. doi:10.1016/j.energy.2018.04.060

[11] S. K. Ayyappa, D. N. Gaonkar, "Performance analysis of a variable-speed wind and fuel cell-based hybrid distributed generation system in grid-connected mode of operation," Electric Power Components and Systems, vol. 44, no. 2, pp. 142-151, Jan. 2016. doi:10.1080/15325008.2015.1102988

[12] T. Ma, M. H. Cintuglu, O. A. Mohammed, "Control of a hybrid AC/DC microgrid involving energy storage and pulsed loads," IEEE Transactions on Industry Applications, vol. 53, no. 1, pp. 567-575, Jan. 2017. doi:10.1109/TIA.2016.2613981

[13] A. A. Abdelsalam, H. A. Gabbar, A. M. Sharaf, "Performance enhancement of hybrid AC/DC microgrid based D-FACTS," International Journal of Electrical Power & Energy Systems, vol. 63, pp. 382-393, Dec. 2014. doi:10.1016/j.ijepes.2014.06.003

[14] C. K. Sundarabalan, K. Selvi, "Real coded GA optimized fuzzy logic controlled PEMFC based Dynamic Voltage Restorer for reparation of voltage disturbances in distribution system," International Journal of Hydrogen Energy, vol. 42, no. 1, pp. 603-613, Jan. 2017. doi:10.1016/j.ijhydene.2016.09.061

[15] R. Eberhart, J. Kennedy, "A new optimizer using particle swarm theory," Proceedings of the Sixth International Symposium on Micro Machine and Human Science, IEEE, Nagoya, Japan, Oct. 1995, pp. 39-43. doi:10.1109/MHS.1995.494215

[16] N. Bigdeli, "Optimal management of hybrid PV/fuel cell/battery power system: A comparison of optimal hybrid approaches," Renewable and Sustainable Energy Reviews, vol. 42, pp. 377-393, Feb. 2015. doi:10.1016/j.rser.2014.10.032

[17] L. K. Letting, J. L. Munda, Y. Hamam, "Optimization of a fuzzy logic controller for PV grid inverter control using S-function based PSO," Solar Energy, vol. 86, no. 6, pp. 1689-1700, Jun. 2012. DOI:10.1016/j.solener.2012.03.018

[18] D. Fister, I. Fister Jr, I. Fister, R. Safaric, "Parameter tuning of PID controller with reactive nature-inspired algorithms," Robotics and Autonomous Systems, vol. 84, pp. 64-75, Oct. 2016. doi:10.1016/j.robot.2016.07.005

[19] M. G. Villarreal-Cervantes, J. Alvarez-Gallegos, "Off-line PID control tuning for a planar parallel robot using DE variants," Expert Systems with Applications, vol. 64, pp. 444-454. Dec. 2016. doi:10.1016/j.eswa.2016.08.013

[20] W. Bai, M. R. Abedi, K. Y. Lee, "Distributed generation system control strategies with PV and fuel cell in microgrid operation," Control Engineering Practice, vol. 53, pp.184-193, Aug. 2016. doi:10.1016/j.conengprac.2016.02.002

[21] P. García-Trivino, A. J. Gil-Mena, F. Llorens-Iborra, C. A. García-Vazquez, L.M. Fernández-Ramírez, F. Jurado, "Power control based on particle swarm optimization of grid-connected inverter for hybrid renewable energy system," Energy Conversion and Management, vol. 91, pp. 83-92, Feb. 2015. doi:10.1016/j.enconman.2014.11.051

[22] M. S. Kiran, "Particle swarm optimization with a new update mechanism," Applied Soft Computing, vol. 60, pp. 670-678. Nov. 2017. doi:10.1016/j.asoc.2017.07.050

[23] T. Kalitjuka, "Control of voltage source converters for power system applications (Master's thesis, Institutt for elkraftteknikk)" 2011.

[24] C. Bajracharya, M. Molinas, J. A. Suul, T. M. Undeland, "Understanding of tuning techniques of converter controllers for VSC-HVDC," Nordic Workshop on Power and Industrial Electronics (NORPIE), Espoo, Finland, Jun. 2008, Helsinki University of Technology.

[25] T. Vigneysh, N. Kumarappan, "Autonomous operation and control of photovoltaic/solid oxide fuel cell/battery energy storage based microgrid using fuzzy logic controller," International journal of hydrogen energy, vol. 41, no. 3, pp. 1877-1891, Jan. 2016. doi:10.1016/j.ijhydene.2015.11.022

[26] N. S. Jayalakshmi, D. N. Gaonkar, A. Balan, P. Patil, S. A. Raza, "Dynamic modeling and performance study of a stand-alone photovoltaic system with battery supplying dynamic load," International Journal of Renewable Energy Research (IJRER), vol. 4, no. 3, pp. 635-640, Sep. 2014.

[27] O. C. Onar, M. Uzunoglu, M. S. Alam, "Dynamic modeling, design and simulation of a wind/fuel cell/ultra-capacitor-based hybrid power generation system," Journal of power sources, vol. 161, no. 1, pp. 707-722, Oct. 2006. doi:10.1016/j.jpowsour.2006.03.055

[28] N. S. Jayalakshmi, D. N. Gaonkar, "Maximum power point tracking for grid integrated variable speed wind based DG system with dynamic load," International Journal of Renewable Energy Research (IJRER), vol. 4, no. 2, pp. 464-470, Jun. 2014.

[29] T. Back, "Evolutionary algorithms in theory and practice: evolution strategies, evolutionary programming, genetic algorithms," Oxford university press, Jan. 1996.

[30] D. Karaboga, "An idea based on honey bee swarm for numerical optimization," Technical report-tr06, Erciyes university, engineering faculty, computer engineering department. Oct. 2005.